

Lifted contact dynamics for efficient direct optimal control of rigid body systems with contacts

Sotaro Katayama¹ and Toshiyuki Ohtsuka¹

Abstract—We propose a novel and efficient lifting approach for the direct optimal control of rigid-body systems with contacts to improve the convergence properties of Newton-type methods. To relax the high nonlinearity, we consider all variables, including the state, acceleration, contact forces, and control input torques, as optimization variables and the inverse dynamics and acceleration-level contact constraints as equality constraints. We eliminate the update of the acceleration, contact forces, and their dual variables from the linear equation to be solved in each Newton-type iteration in an efficient manner. As a result, the computational cost per Newton-type iteration is almost identical to that of the conventional non-lifted Newton-type iteration that embeds contact dynamics in the state equation. We conducted numerical experiments on the whole-body optimal control of various quadrupedal gaits subject to the friction cone constraints considered in interior-point methods and demonstrated that the proposed method can significantly increase the convergence speed to more than twice that of the conventional non-lifted approach.

I. INTRODUCTION

Trajectory optimization (TO) and model predictive control (MPC) are promising frameworks for motion planning and control of rigid-body systems that make rigid contacts with the environment, e.g., legged robots and robot manipulators, whose dynamics are highly nonlinear and include discontinuities. The computational time required to solve optimal control problems (OCPs) remains a critical constraint for using these two schemes, particularly MPC. The solution methods of such OCPs are generally classified into two types: contact-implicit and event-driven approaches.

Contact-implicit approaches aim to determine the optimal trajectory without specifying the contact sequence in advance. The simplest approach is to approximate the contact forces using spring-damper systems [1]; however, it lacks accuracy and involves stiff optimization problems. The same problem typically occurs in other smooth soft-contact models such as in [2].

A more accurate approach is the time-stepping method [3], which approximates the impact forces using small time steps, yielding mathematical programs with complementarity constraints (MPCC) [4] or bilevel optimization problems [5]. However, their non-smooth nature typically requires several iterations compared with the smooth OCPs [4], [5]. Moreover, some theoretical and practical challenges remain, e.g., violation of the linear independence constraint qualification (LICQ) and suspicious stationary points [6].

In contrast, event-driven approaches formulate the OCPs under predefined contact sequences and model the impacts between the system and the environment explicitly via Newton’s law of impact. Therefore, event-driven approaches are more accurate and the continuous-time OCP can be discretized with coarser grids than in contact-implicit methods, which means that they can be faster. Moreover, they consist of only smooth optimization problems; therefore, we can solve them efficiently using the off-the-shelf Newton-type methods for smooth OCPs without being overly cautious with the LICQ. Although event-driven approaches cannot optimize contact sequences as contact-implicit methods can, they can optimize the instants of the impacts under a given contact sequence, as studied in [7], [8].

The contact-consistent forward dynamics, a calculation of the acceleration and contact forces using the given configuration, velocity, and torques, which we call “contact dynamics,” has been successfully used with Newton-type methods to efficiently solve event-driven OCPs [8], [9], [10], [11]. [9] combined contact dynamics with the direct multiple shooting method (DMS) [12]. [10] and [8] combined contact dynamics with the iterative linear quadratic regulator (iLQR) [13]. [11] improved the approach of [10] using the efficient analytical derivatives proposed in [14] to compute the sensitivities of contact dynamics. However, such an approach still contains high nonlinearity, which results in slow convergence, particularly when there are costs and constraints on the contact forces, e.g., friction cone constraints.

The lifted Newton method is a promising option to relax such high nonlinearity. It involves adding intermediate variables and lifting the optimization problem into a higher-dimensional one [15]. For example, it is well known in the context of numerical optimal control and MPC that the multiple shooting method, which considers the state and control input as the optimization variables, has preferred convergence properties over the single shooting method, which considers only the control input as the optimization variable [12]. However, to the best of our knowledge, no lifting method has previously been used to efficiently treat the contact forces in event-driven OCPs. For example, our previous study [16] considered the contact forces and acceleration as the optimization variables, as well as the state and control input. However, a large dimension of the contact constraint can result in inefficiency because the size of the linear equation to be solved in each Newton-type iteration increases in proportion to the number of contacts. Moreover, that study did not consider the impulse dynamics, which is necessary to formulate event-driven OCPs.

¹S. Katayama and T. Ohtsuka are with the Department of System Science, Graduate School of Informatics, Kyoto University, Kyoto, Japan. katayama.25w@st.kyoto-u.ac.jp, ohtsuka@i.kyoto-u.ac.jp

In this paper, we propose *lifted contact dynamics*, a novel and efficient lifting approach for the direct optimal control of rigid-body systems with contacts to improve the convergence properties of Newton-type methods. To relax the high nonlinearity, we consider all variables, including the state, acceleration, contact forces, and control input torques, as the optimization variables and the inverse dynamics and acceleration-level contact constraints as equality constraints. We eliminate the updating of the acceleration, contact forces, and their dual variables from the linear equation to be solved in each Newton-type iteration in an efficient manner. As a result, the computational cost per Newton-type iteration is almost identical to that of the conventional non-lifted Newton-type iteration that embeds contact dynamics in the state equation. This aspect distinguishes this study from our previous method [16], which was inefficient for high-dimensional contact constraints. We also propose a similar lifting method for impulse dynamics, which was not considered in our previous study [16]. We conducted numerical experiments on the whole-body optimal control of various quadrupedal gaits subject to the friction cone constraints considered in the interior-point methods and demonstrated that the proposed method can significantly increase the convergence speed to more than twice that of conventional approaches based on the non-lifted contact dynamics.

The remainder of this paper is organized as follows. In Section II, we review the contact and impulse dynamics and conventional formulations of event-driven OCPs. In Section III, we introduce the lifted contact dynamics, a Newton-type method that efficiently condenses the linear equations to be solved in each Newton iteration. Section IV compares the proposed method with existing approaches based on the non-lifted contact dynamics and demonstrates its effectiveness in terms of the convergence properties. Section V concludes the paper and outlines future research directions.

Notation: We denote the partial derivatives of a differentiable function with certain variables using a function with subscripts; i.e., $f_x(x)$ denotes $\frac{\partial f}{\partial x}(x)$ and $g_{xy}(x, y)$ denotes $\frac{\partial^2 g}{\partial x \partial y}(x, y)$. We denote an $n \times n$ identity matrix as I_n .

II. OVERVIEW OF OPTIMAL CONTROL PROBLEMS OF RIGID-BODY SYSTEMS WITH CONTACTS

A. Contact dynamics

First, we review the components to formulate event-driven direct OCPs, e.g., the contact dynamics and discretized state equations. Let Q be the configuration manifold of the rigid-body system. Let $q \in Q$, $v \in \mathbb{R}^n$, $a \in \mathbb{R}^n$, $f \in \mathbb{R}^{n_f}$, and $u \in \mathbb{R}^m$ be the configuration, generalized velocity, acceleration, stack of the contact forces, and joint torques, respectively. The equation of motion of the rigid-body system is expressed as

$$M(q)a + h(q, v) - J^T(q)f = S^T u, \quad (1)$$

where $M(q) \in \mathbb{R}^{n \times n}$ denotes the inertia matrix, $h(q, v) \in \mathbb{R}^n$ encompasses the Coriolis, centrifugal, and gravitational terms, $J(q) \in \mathbb{R}^{n_f \times n}$ denotes the stack of the contact Jacobians, and $S \in \mathbb{R}^{m \times n}$ denotes the selection matrix. The

evolution of the state $[q^T \ v^T]^T$ with time step $\Delta\tau > 0$ is expressed as

$$\begin{bmatrix} q^+ \\ v^+ \end{bmatrix} = \begin{bmatrix} q \oplus v\Delta\tau \\ v + a\Delta\tau \end{bmatrix}, \quad (2)$$

where \oplus denotes the increment operator on the configuration manifold Q [17]. We formulate the OCPs based on the DMS and then consider an equivalent equality constraint:

$$\begin{bmatrix} \delta(q, q^+) + v\Delta\tau \\ v - v^+ + a\Delta\tau \end{bmatrix} = 0, \quad (3)$$

where $\delta(q_1, q_2) := q_1 \ominus q_2 \in \mathbb{R}^n$, and \ominus denotes the subtraction operator between the two configurations [17]. The system also satisfies the contact constraints of the form

$$\mathbf{p}(q) = 0, \quad (4)$$

where $\mathbf{p}(q) \in \mathbb{R}^{n_f}$ is the stack of the positions of the contact frames. In event-driven OCPs, instead of considering (4) over a time interval, we typically consider the acceleration-level constraint over the time interval that is generalized into the form of Baumgarte's stabilization method [18]:

$$\mathbf{a}(q, v, a) := \ddot{\mathbf{p}} + 2\alpha\dot{\mathbf{p}} + \beta^2\mathbf{p} = J(q)a + \mathbf{b}(q, v), \quad (5)$$

where α and β are weight parameters, and we define

$$\mathbf{b}(q, v) := \dot{J}(q, v)v + 2\alpha J(q)v + \beta^2\mathbf{p}(q). \quad (6)$$

By setting $\alpha = \beta > 0$, we can stabilize the violation of the original constraint (4) over the time interval provided that (4) and the equality constraint on the contact velocity,

$$\dot{\mathbf{p}}(q, v) = J(q)v = 0, \quad (7)$$

are satisfied at a point on the interval [19]. Note that (5) is reduced to the equality constraint on the acceleration of the contact frames with $\alpha = \beta = 0$. By combining (1) and (5), we obtain the contact dynamics, i.e., the contact-consistent forward dynamics:

$$\begin{bmatrix} M(q) & J^T(q) \\ J(q) & O \end{bmatrix} \begin{bmatrix} a \\ -f \end{bmatrix} = \begin{bmatrix} S^T u - h(q, v) \\ -\mathbf{b}(q, v) \end{bmatrix}. \quad (8)$$

In the conventional approaches [8], [9], [10], [11], we eliminate a and f from the OCP using (8). For example, we substitute a with (8) in (2) or (3) and consider these equations to be the discretized state equation. We can also eliminate a and f from the cost function and the constraints, e.g., the friction cone constraints, using (8).

B. Impulse dynamics

Similar to the contact dynamics, the equation of Newton's law of impact of the systems is expressed as

$$M(q)\delta v - J^T(q)\Lambda = 0, \quad (9)$$

where $\delta v \in \mathbb{R}^n$ denotes the impulse change in the generalized velocity, and $\Lambda \in \mathbb{R}^{n_f}$ denotes the stack of the impact forces. The evolution of the state between the impulse is expressed as

$$\begin{bmatrix} q^+ \\ v^+ \end{bmatrix} = \begin{bmatrix} q \\ v + \delta v \end{bmatrix}. \quad (10)$$

Our formulation based on the DMS considers an equivalent equality constraint:

$$\begin{bmatrix} \delta(q, q^+) \\ v - v^+ + \delta v \end{bmatrix} = 0. \quad (11)$$

Herein, we assume a completely inelastic collision, which results in the contact velocity constraints of the form (7) immediately after the impulse as

$$\mathbf{v}(q, v, \delta v) := \dot{\mathbf{p}}(q, v + \delta v) = J(q)(v + \delta v) = 0. \quad (12)$$

The contact position constraint (4) for the frames with impacts is also imposed at the impulse instant. By combining (9) and (12), we obtain the impulse dynamics:

$$\begin{bmatrix} M(q) & J^T(q) \\ J(q) & O \end{bmatrix} \begin{bmatrix} \delta v \\ -\Lambda \end{bmatrix} = \begin{bmatrix} 0 \\ -J(q)v \end{bmatrix}. \quad (13)$$

In the conventional formulation, as well as the contact dynamics, δv and Λ are eliminated from the OCP using (13), for example, from (10) and (11).

C. Conventional formulation of direct optimal control

The conventional formulation of the direct optimal control of rigid-body systems with N discretization grids is summarized as follows [8], [9], [10], [11]: determine the $q_0, \dots, q_N \in Q$, $v_0, \dots, v_N \in \mathbb{R}^n$, and $\{u_i\}_{i \in \mathcal{I}} \in \mathbb{R}^m$ that minimize a given cost function

$$J := \varphi(x_N) + \sum_{i \in \mathcal{I}} l(x_i, u_i, a_i, f_i) + \sum_{j \in \mathcal{J}} l(x_j, \delta v_j, \Lambda_j), \quad (14)$$

where $x_i := [q_i^T \ v_i^T]^T$ is the state, $\mathcal{J} \subset \{0, \dots, N-1\}$ is the set of the impulse stages, and $\mathcal{I} := \{0, \dots, N-1\} \setminus \mathcal{J}$, subject to the state equation obtained by eliminating a_i from (2) using (8), the state equation at the impulse obtained by eliminating δv_j from (10) using (13), the contact-position constraint (4) at the impulse instant, and the other user-defined equality and inequality constraints. Moreover, a_i , f_i , δv_j , and Λ_j are also eliminated from the cost function (14) and the constraints other than the state equations, which increases the nonlinearity of the OCPs. In [9], this problem was solved using the DMS, that is, x_0, \dots, x_N and $\{u_i\}_{i \in \mathcal{I}}$ were considered as the optimization variables, the state equations were considered as the equality constraints, and (14) was represented by x_0, \dots, x_N and $\{u_i\}_{i \in \mathcal{I}}$. In [8], [10], [11], this problem was solved using the single shooting method, that is, x_0, \dots, x_N were further eliminated from the optimization problem using the state equations, and only $\{u_i\}_{i \in \mathcal{I}}$ were considered as the decision variables, e.g., (14) was represented only by $\{u_i\}_{i \in \mathcal{I}}$.

III. LIFTED CONTACT DYNAMICS IN DIRECT OPTIMAL CONTROL

A. Lifted contact dynamics

We herein present the lifted contact dynamics to relax the high nonlinearity in OCPs. Let $i \in \mathcal{I}$, $y_i := (q_i, v_i, a_i, f_i)$, and $z_i := (q_i, v_i, a_i)$. We first augment the control input to

convert the system into a fully actuated system in the numerical optimization. Without loss of generality, we assume that S is given by $[O \ I]^T$, and we define

$$\tilde{u}_i := \begin{bmatrix} u_i^0 \\ u_i \end{bmatrix}, \quad (15)$$

where $u_i^0 \in \mathbb{R}^{n-m}$ denotes the virtual torques on the passive joints. Thus, we can express (1) as an equality constraint of the inverse dynamics as follows:

$$\text{ID}(y_i) - \tilde{u}_i = 0, \quad (16)$$

where $\text{ID}(y_i)$ is defined by the left-hand side of (1) and can be computed efficiently using the recursive Newton–Euler algorithm (RNEA) [20], a fast algorithm for inverse dynamics, with an additional equality constraint

$$u_i^0 = \bar{S}^T \tilde{u}_i = 0, \quad (17)$$

where $\bar{S} := [I \ O]^T \in \mathbb{R}^{n \times n-m}$ is the passive selection matrix. We consider a_i and f_i as the optimization variables and (1), (5), and (17) as the equality constraints. The first-order derivatives of the Lagrangian \mathcal{L} (defined by augmenting the constraints to the cost function (14)) with respect to the variables at the stage i , that is, the part of the Karush–Kuhn–Tucker (KKT) conditions associated with the stage i , are given by (3), (16), (5), and (17),

$$\begin{bmatrix} \mathcal{L}_{q_i}^T \\ \mathcal{L}_{v_i}^T \end{bmatrix} = \begin{bmatrix} l_{q_i}^T \\ l_{v_i}^T \end{bmatrix} + \begin{bmatrix} \delta_{q_i}^T(q_i, q_{i+1}) & O \\ I_n \Delta \tau & I_n \end{bmatrix} \begin{bmatrix} \lambda_{i+1} \\ \gamma_{i+1} \end{bmatrix} \\ + \begin{bmatrix} \text{ID}_{q_i}^T(y_i) & \mathbf{a}_{q_i}^T(z_i) \\ \text{ID}_{v_i}^T(y_i) & \mathbf{a}_{v_i}^T(z_i) \end{bmatrix} \begin{bmatrix} \beta_i \\ \mu_i \end{bmatrix} \Delta \tau + \begin{bmatrix} \delta_{q_i}^T(q_{i-1}, q_i) \lambda_i \\ -\gamma_i \end{bmatrix} = 0, \quad (18)$$

$$\begin{bmatrix} \mathcal{L}_{a_i}^T \\ -\mathcal{L}_{f_i}^T \end{bmatrix} = \begin{bmatrix} l_{a_i}^T \\ -l_{f_i}^T \end{bmatrix} + \begin{bmatrix} \gamma_{i+1} \Delta \tau \\ 0 \end{bmatrix} \\ + \begin{bmatrix} \text{ID}_{a_i}^T(y_i) & \mathbf{a}_{a_i}^T(z_i) \\ -\text{ID}_{f_i}^T(y_i) & -\mathbf{a}_{f_i}^T(z_i) \end{bmatrix} \begin{bmatrix} \beta_i \\ \mu_i \end{bmatrix} \Delta \tau = 0, \quad (19)$$

and

$$\mathcal{L}_{\tilde{u}_i}^T := l_{\tilde{u}_i}^T - \beta_i \Delta \tau + \bar{S}^T \nu_i \Delta \tau = 0, \quad (20)$$

where $\lambda_{i+1}, \gamma_{i+1}, \beta_i \in \mathbb{R}^n$, $\mu_i \in \mathbb{R}^{n_f}$, and $\nu \in \mathbb{R}^{n-m}$ are the Lagrange multipliers with respect to (3), (16), (5), and (17), respectively.

In the Newton-type methods, these KKT conditions are linearized into linear equations with respect to the Newton directions Δq_i , Δv_i , Δa_i , Δf_i , Δu_i , Δu_i^0 , $\Delta \lambda_{i+1}$, $\Delta \gamma_{i+1}$, $\Delta \beta_i$, $\Delta \mu_i$, and $\Delta \nu_i$. However, this problem is significantly larger than the conventional OCPs based on the non-lifted contact dynamics that considers only Δq_i , Δv_i , Δu_i , $\Delta \lambda_{i+1}$, and $\Delta \gamma_{i+1}$. Thus, we propose an efficient condensing method to reduce the size of the linear equation. We first observe that the equality constraints (16) and (5) are linearized as

$$\begin{bmatrix} M(q_i) & J^T(q_i) \\ J(q_i) & O \end{bmatrix} \begin{bmatrix} \Delta a_i \\ -\Delta f_i \end{bmatrix} \\ = - \begin{bmatrix} \text{ID}_{q_i}(y_i) & \text{ID}_{v_i}(y_i) \\ \mathbf{a}_{q_i}(z_i) & \mathbf{a}_{v_i}(z_i) \end{bmatrix} \begin{bmatrix} \Delta q_i \\ \Delta v_i \end{bmatrix} + \begin{bmatrix} \Delta \tilde{u}_i \\ 0 \end{bmatrix} - \begin{bmatrix} \text{ID}(y_i) \\ \mathbf{a}(z_i) \end{bmatrix}. \quad (21)$$

Moreover, we always set $u_i^0 = 0$ and obtain from (17)

$$\Delta u_i^0 = -u_i^0 = 0. \quad (22)$$

Therefore, we can express Δa_i and Δf_i using the linear combinations of Δq_i , Δv_i , and Δu_i using (21) and (22) if we compute

$$\begin{bmatrix} M(q_i) & J^T(q_i) \\ J(q_i) & O \end{bmatrix}^{-1}. \quad (23)$$

Next, we observe that (19) and (20) are linearized into

$$\begin{aligned} & \begin{bmatrix} \mathcal{L}_{a_i}^T \\ -\mathcal{L}_{f_i}^T \end{bmatrix} + \begin{bmatrix} \mathcal{L}_{a_i y_i} \\ -\mathcal{L}_{f_i y_i} \end{bmatrix} \Delta y_i + \begin{bmatrix} \Delta \gamma_{i+1} \Delta \tau \\ O \end{bmatrix} \\ & + \begin{bmatrix} M(q_i) & J^T(q_i) \\ J(q_i) & O \end{bmatrix} \begin{bmatrix} \Delta \beta_i \\ \Delta \mu_i \end{bmatrix} \Delta \tau = 0 \end{aligned} \quad (24)$$

and

$$\mathcal{L}_{u_i y_i}^T \Delta y_i - \Delta \beta_i \Delta \tau + \bar{S} \Delta \nu_i \Delta \tau = 0. \quad (25)$$

Therefore, we can also express the Newton directions of the dual variables $\Delta \beta_i$, $\Delta \mu_i$, and $\Delta \nu_i$ with the linear combinations of Δq_i , Δv_i , Δu_i , and $\Delta \gamma_{i+1}$ using (24) and (25) if we compute (23). Subsequently, the linear equations to be solved in the Newton-type iterations at stage i are reduced to that with respect to Δq_i , Δv_i , Δu_i , $\Delta \lambda_{i+1}$, and $\Delta \gamma_{i+1}$, defined as

$$\begin{aligned} & \begin{bmatrix} \tilde{F}_{q,i} \\ \tilde{F}_{v,i} \end{bmatrix} + \begin{bmatrix} \delta_{q_i}(q_i, q_{i+1}) & I \Delta \tau \\ \tilde{F}_{v q,i} & \tilde{F}_{v v,i} \end{bmatrix} \begin{bmatrix} \Delta q_i \\ \Delta v_i \end{bmatrix} + \begin{bmatrix} O \\ \tilde{F}_{v u,i} \end{bmatrix} \Delta u_i \\ & + \begin{bmatrix} \delta_{q_{i+1}}(q_i, q_{i+1}) & O \\ O & -I \end{bmatrix} \begin{bmatrix} \Delta q_{i+1} \\ \Delta v_{i+1} \end{bmatrix} = 0 \end{aligned} \quad (26)$$

$$\begin{aligned} & \begin{bmatrix} \tilde{\mathcal{L}}_{q_i}^T \\ \tilde{\mathcal{L}}_{v_i}^T \end{bmatrix} + \begin{bmatrix} \tilde{\mathcal{L}}_{q_i q_i} & \tilde{\mathcal{L}}_{q_i v_i} \\ \tilde{\mathcal{L}}_{v_i q_i} & \tilde{\mathcal{L}}_{v_i v_i} \end{bmatrix} \begin{bmatrix} \Delta q_i \\ \Delta v_i \end{bmatrix} + \begin{bmatrix} \tilde{\mathcal{L}}_{q_i u_i} \\ \tilde{\mathcal{L}}_{v_i u_i} \end{bmatrix} \Delta u_i \\ & + \begin{bmatrix} \delta_{q_i}^T(q_i, q_{i+1}) & \tilde{F}_{v q,i} \\ I_n \Delta \tau & \tilde{F}_{v v,i} \end{bmatrix} \begin{bmatrix} \Delta \lambda_{i+1} \\ \Delta \gamma_{i+1} \end{bmatrix} \\ & + \begin{bmatrix} \delta_{q_i}^T(q_{i-1}, q_i) \Delta \lambda_i \\ -\Delta \gamma_i \end{bmatrix} = 0, \end{aligned} \quad (27)$$

and

$$\tilde{\mathcal{L}}_{u_i}^T + \begin{bmatrix} \tilde{\mathcal{L}}_{q_i u_i} & \tilde{\mathcal{L}}_{v_i u_i} \end{bmatrix} \begin{bmatrix} \Delta q_i \\ \Delta v_i \end{bmatrix} + \tilde{\mathcal{L}}_{u_i u_i} \Delta u_i + \tilde{F}_{v u,i} \Delta \gamma_{i+1} = 0, \quad (28)$$

where the vectors and matrices with a superscript tilde are derived via simple additions and multiplications of the original Hessians of the Lagrangian, Jacobians of the constraints, and residuals in the KKT conditions. We omit their definitions here because they are excessively long, but they are easy to derive. Note that our previous approach [16] involves solving the linear equation with respect to Δq_i , Δv_i , Δa_i , Δf_i , $\Delta \mu_i$, and $\Delta \nu_i$; thus, it can be inefficient compared with the proposed method. After solving the linear equations and obtaining Δq_i , Δv_i , Δu_i , $\Delta \lambda_{i+1}$, and $\Delta \gamma_{i+1}$, we can easily compute Δa_i , Δf_i , $\Delta \beta_i$, and $\Delta \mu_i$ using (21) and (24), which is called an expansion procedure.

B. Lifted impulse dynamics

Next, we present the lifted impulse dynamics. Let $j \in \mathcal{J}$, $y_j := (q_j, v_j, \delta v_j, \Lambda_j)$, and $z_j := (q_j, v_j, \delta v_j)$. We express (9) as an equality constraint:

$$\Gamma(y_j) = 0, \quad (29)$$

where $r(y_i)$ is defined by the left-hand side of (9). We consider δv_j and Λ_j as the optimization variables and (29) and (7) as the equality constraints. The first-order derivatives of the Lagrangian \mathcal{L} with respect to the variables at the stage of impulse j , that is, the part of the KKT conditions associated with the impulse stage j , are given by (11), (29), (7),

$$\begin{aligned} & \begin{bmatrix} \mathcal{L}_{q_j}^T \\ \mathcal{L}_{v_j}^T \end{bmatrix} = \begin{bmatrix} l_{q_j}^T \\ l_{v_j}^T \end{bmatrix} + \begin{bmatrix} \delta_{q_j}^T(q_j, q_{j+1}) & O \\ O & I_n \end{bmatrix} \begin{bmatrix} \lambda_{j+1} \\ \gamma_{j+1} \end{bmatrix} \\ & + \begin{bmatrix} \Gamma_{q_j}^T(y_j) & \mathbf{v}_{q_j}^T(z_j) \\ \Gamma_{v_j}^T(y_j) & \mathbf{v}_{v_j}^T(z_j) \end{bmatrix} \begin{bmatrix} \beta_j \\ \mu_j \end{bmatrix} + \begin{bmatrix} \delta_{q_j}^T(q_{j-1}, q_j) \lambda_j \\ -\gamma_j \end{bmatrix} = 0, \end{aligned} \quad (30)$$

and

$$\begin{aligned} & \begin{bmatrix} \mathcal{L}_{\delta v_j}^T \\ -\mathcal{L}_{\Lambda_j}^T \end{bmatrix} = \begin{bmatrix} l_{\delta v_j}^T \\ -l_{\Lambda_j}^T \end{bmatrix} + \begin{bmatrix} \gamma_{j+1} \\ 0 \end{bmatrix} \\ & + \begin{bmatrix} \Gamma_{a_j}^T(\tilde{y}_j) & \mathbf{v}_{\delta v_j}^T(z_j) \\ -\Gamma_{f_j}^T(\tilde{y}_j) & -\mathbf{v}_{f_j}^T(z_j) \end{bmatrix} \begin{bmatrix} \beta_j \\ \mu_j \end{bmatrix} = 0, \end{aligned} \quad (31)$$

where $\lambda_{j+1}, \gamma_{j+1}, \beta_j \in \mathbb{R}^n$, and $\mu_j \in \mathbb{R}^{n_f}$ are the Lagrange multipliers with respect to (11), (29), and (7), respectively.

These KKT conditions are also linearized into linear equations with respect to the Newton directions Δq_i , Δv_i , $\Delta \delta v_i$, $\Delta \Lambda_i$, $\Delta \lambda_{i+1}$, $\Delta \gamma_{i+1}$, $\Delta \beta_i$, and $\Delta \mu_i$, which are larger than those of the non-lifted counterpart with respect to Δq_i , Δv_i , $\Delta \lambda_{i+1}$, and $\Delta \gamma_{i+1}$. Thus, we propose an efficient condensing method to reduce the size of the linear equation. We first observe that the equality constraints (29) and (7) are linearized as

$$\begin{aligned} & \begin{bmatrix} M(q_j) & J^T(q_j) \\ J(q_j) & O \end{bmatrix} \begin{bmatrix} \Delta \delta v_j \\ -\Delta \Lambda_j \end{bmatrix} \\ & = - \begin{bmatrix} \Gamma_{q_j}(y_j) & \Gamma_{v_j}(y_j) \\ \mathbf{v}_{q_j}(z_j) & \mathbf{v}_{v_j}(z_j) \end{bmatrix} \begin{bmatrix} \Delta q_j \\ \Delta v_j \end{bmatrix} - \begin{bmatrix} \Gamma(y_j) \\ \mathbf{v}(z_j) \end{bmatrix}. \end{aligned} \quad (32)$$

Therefore, we can express $\Delta \delta v_j$ and $\Delta \Lambda_j$ with the linear combinations of Δq_j and Δv_j if we compute (23) for q_j . Next, we observe that (31) is linearized into

$$\begin{aligned} & \begin{bmatrix} \mathcal{L}_{\delta v_j}^T \\ -\mathcal{L}_{\Lambda_j}^T \end{bmatrix} + \begin{bmatrix} \mathcal{L}_{\delta v_j y_j} \\ -\mathcal{L}_{\Lambda_j y_j} \end{bmatrix} \Delta y_j + \begin{bmatrix} \Delta \gamma_{j+1} \\ 0 \end{bmatrix} \\ & + \begin{bmatrix} M(q_j) & J^T(q_j) \\ J(q_j) & O \end{bmatrix} \begin{bmatrix} \Delta \beta_j \\ \Delta \mu_j \end{bmatrix} = 0. \end{aligned} \quad (33)$$

Therefore, we can also express the Newton directions of the dual variables $\Delta \beta_j$ and $\Delta \mu_j$ with the linear combinations of Δq_j , Δv_j , and $\Delta \gamma_{j+1}$ if we solve (23) for q_j . Subsequently, the linear equations to be solved in the Newton-type iterations are reduced with respect to Δq_j , Δv_j , $\Delta \lambda_{j+1}$, and

$\Delta\gamma_{j+1}$ and are expressed as

$$\begin{aligned} & \begin{bmatrix} \tilde{F}_{q,j} \\ \tilde{F}_{v,j} \end{bmatrix} + \begin{bmatrix} \delta_{q_j}(q_j, q_{j+1}) & O \\ F_{vq,j} & \tilde{F}_{vv,j} \end{bmatrix} \begin{bmatrix} \Delta q_j \\ \Delta v_j \end{bmatrix} \\ & + \begin{bmatrix} \delta_{q_{j+1}}(q_j, q_{j+1}) & O \\ O & -I \end{bmatrix} \begin{bmatrix} \Delta q_{j+1} \\ \Delta v_{j+1} \end{bmatrix} = 0 \end{aligned} \quad (34)$$

and

$$\begin{aligned} & \begin{bmatrix} \tilde{\mathcal{L}}_{q_j}^T \\ \tilde{\mathcal{L}}_{v_j}^T \end{bmatrix} + \begin{bmatrix} \tilde{\mathcal{L}}_{q_j q_j} & \tilde{\mathcal{L}}_{q_j v_j} \\ \tilde{\mathcal{L}}_{v_j q_j} & \tilde{\mathcal{L}}_{v_j v_j} \end{bmatrix} \begin{bmatrix} \Delta q_j \\ \Delta v_j \end{bmatrix} \\ & + \begin{bmatrix} \delta_{q_j}^T(q_j, q_{j+1}) & \tilde{F}_{vq,j} \\ O & \tilde{F}_{vv,j} \end{bmatrix} \begin{bmatrix} \Delta \lambda_{j+1} \\ \Delta \gamma_{j+1} \end{bmatrix} \\ & + \begin{bmatrix} \delta_{q_j}^T(q_{j-1}, q_j) \Delta \lambda_j \\ -\Delta \gamma_j \end{bmatrix} = 0, \end{aligned} \quad (35)$$

for which we omit the definitions of the terms with a superscript tilde because they are easy to derive similar to those of the lifted contact dynamics. After solving the linear equations and obtaining Δq_j , Δv_j , $\Delta \lambda_{j+1}$, and $\Delta \gamma_{j+1}$, we can easily compute $\Delta \delta v_j$, $\Delta \lambda_j$, $\Delta \beta_j$, and $\Delta \mu_j$ using (32) and (33), which is the expansion procedure of the impulse stage.

C. Riccati recursion for LQR subproblem

The above condensed linear equations can be considered as the KKT conditions of an LQR subproblem with the state Δx_i and control input Δu_i , and we can solve them only with $O(N)$ complexity using the Riccati recursion [21], whereas the direct Cholesky factorization requires an $O(N^3)$ computational burden. For example, iLQR and differential dynamic programming (DDP), which use the Riccati recursion for single-shooting OCPs with nonlinear forward pass, can efficiently solve very large-scale problems [1], [10], [11].

D. Primal-dual interior-point method for inequality constraints

OCPs of rigid-body systems can contain many inequality constraints, e.g., joint angle limits, joint angular velocity limits, joint torque limits, and friction cones. Thus, we use the primal-dual interior-point method [22] to efficiently solve the many inequality constraints including nonlinear ones. In the primal-dual interior-point method, only certain terms related to the second- and first-order derivatives of the logarithmic barrier functions are added to the Hessians $\mathcal{L}_{y_i y_i}$ and residuals \mathcal{L}_{y_i} , respectively, and there are no effects on the proposed condensing method and the LQR subproblem. That is, none of the constraints due to the inequality constraints are added to the LQR subproblem, and we can apply the Riccati recursion algorithm. After solving the LQR subproblem and obtaining the direction Δy_i , we can efficiently compute the directions of the slack variables and Lagrange multipliers of the inequality constraints. Detailed explanations on the primal-dual interior-point method are available in [22], [23].

Algorithm 1 Computation of the Newton direction using the lifted contact dynamics

Input: Initial state $x(t_0)$, the current solution y_0, \dots, y_{N-1} , q_N , v_N , $\{u_i\}_{i \in \mathcal{I}}$, $\lambda_0, \dots, \lambda_N$, $\gamma_0, \dots, \gamma_N$, $\beta_0, \dots, \beta_{N-1}$, μ_0, \dots, μ_{N-1} , and $\{\nu_i\}_{i \in \mathcal{I}}$

Output: Newton directions $\Delta y_0, \dots, \Delta y_{N-1}$, Δq_N , Δv_N , $\{\Delta u_i\}_{i \in \mathcal{I}}$, $\Delta \lambda_0, \dots, \Delta \lambda_N$, $\Delta \gamma_0, \dots, \Delta \gamma_N$, $\Delta \beta_0, \dots, \Delta \beta_{N-1}$, $\Delta \mu_0, \dots, \Delta \mu_{N-1}$, and $\{\Delta \nu_i\}_{i \in \mathcal{I}}$

- 1: **for** $i = 0, \dots, N$ **do in parallel**
 - 2: Compute the Hessian of the Lagrangian (e.g., $\mathcal{L}_{q_i q_i}$), Jacobians of the constraints (e.g., ID_{q_i} and \mathbf{a}_{q_i}), and residuals in the KKT conditions (e.g., (3), (16), (5), (17), and \mathcal{L}_{q_i}).
 - 3: Compute the matrix inversion (23).
 - 4: Form the condensed Hessians, Jacobians, and KKT residuals (e.g., $\tilde{\mathcal{L}}_{q_i q_i}$, $\tilde{F}_{qq,i}$, and $\tilde{\mathcal{L}}_{q_i}$).
 - 5: **end for**
 - 6: Compute $\Delta q_0, \dots, \Delta q_N$, $\Delta v_0, \dots, \Delta v_N$, $\{\Delta u_i\}_{i \in \mathcal{I}}$, $\Delta \lambda_0, \dots, \Delta \lambda_N$, and $\Delta \gamma_0, \dots, \Delta \gamma_N$ by solving the LQR subproblem, e.g., using the Riccati recursion.
 - 7: **for** $i = 0, \dots, N-1$ **do in parallel**
 - 8: Compute the condensed direction (Δa_i , Δf_i , $\Delta \beta_i$, $\Delta \mu_i$, and $\Delta \nu_i$ for $i \in \mathcal{I}$ or $\Delta \delta v_j$, $\Delta \lambda_j$, $\Delta \beta_j$, and $\Delta \mu_j$ for $j \in \mathcal{J}$).
 - 9: **end for**
-

E. Algorithm

We summarize the single Newton iteration, that is, the computation of the Newton direction of the proposed method, in Algorithm 1. First, we compute the Hessians of the Lagrangian, Jacobians of the constraints, and residuals in the KKT conditions (line 2). The modification of the Hessians and KKT residuals due to the primal-dual interior-point method is also performed in this step. Second, we compute the matrix inversion (23) and form the condensed Hessians, Jacobians, and KKT residuals (lines 3 and 4). These two steps are fully parallelizable because of the multiple-shooting formulation. We then solve the LQR subproblem, e.g., using the Riccati recursion (line 6). Finally, we compute the condensed directions from the solution of the LQR subproblem (line 8). The directions of the slack variables and Lagrange multipliers of the primal-dual interior-point method are also computed in this step.

IV. NUMERICAL EXPERIMENTS: WHOLE-BODY OPTIMAL CONTROL OF QUADRUPEDAL GAITS

A. Experimental settings

To demonstrate the effectiveness of the proposed lifting approach over the conventional non-lifting approaches, we conducted numerical experiments on the whole-body optimal control of a quadrupedal robot called ANYmal [24] for five gaits, that is, walking, trotting, pacing, bounding, and jumping, subject to the friction cone constraints. We considered the polyhedral-approximated friction cone constraint for each

contact force expressed in the world frame $[f_x \ f_y \ f_z]$ as

$$\begin{bmatrix} f_x + \frac{\mu}{\sqrt{2}}f_z \\ -f_x + \frac{\mu}{\sqrt{2}}f_z \\ f_y + \frac{\mu}{\sqrt{2}}f_z \\ -f_y + \frac{\mu}{\sqrt{2}}f_z \\ f_z \end{bmatrix} \geq 0, \quad (36)$$

where $\mu > 0$ is the friction coefficient, and we set it as $\mu = 0.7$. The problem settings of the OCPs for the five gaits are shown in Table I. We compared the following four methods:

- DMS-LCD: DMS based on the proposed lifted contact dynamics
- DMS-CD: DMS based on the conventional non-lifted contact dynamics
- FDDP: Feasibility-driven DDP (FDDP) [11] based on the conventional non-lifted contact dynamics
- iLQR: iLQR based on the conventional non-lifted contact dynamics

where FDDP [11] is a variant of iLQR that improves the numerical robustness by modifying the backward pass of the original iLQR. DMS-LCD and DMS-CD used Gauss–Newton Hessian approximation in computing the Hessians, the primal-dual interior-point method for inequality constraints, and the Riccati recursion to solve the LQR subproblems. Note that the search direction from DMS-CD corresponds to the off-the-shelf nonlinear optimization solvers, e.g., Ipopt [22] applied to the OCPs based on the non-lifted contact dynamics, that is, it corresponds to the approach of [9]. FDDP and iLQR used the relaxed barrier function method (ReB) [25], which is a popular constraint-handling approach in DDP-type methods (e.g., used in [8]). It enables the iteration to lie outside the feasible region but cannot guarantee the feasibility of the optimal solution. We implemented DMS-LCD¹ and DMS-CD in C++ and used `Pinocchio` [26], an efficient C++ library used for rigid-body dynamics and its analytical derivatives, to compute the dynamics and its derivatives of the quadrupedal robot. We used OpenMP [27] for parallel computing (e.g., lines 1–5 of Algorithm 1). For FDDP and iLQR, we used the `Crocodyl` [11] framework, which was also implemented in C++, `Pinocchio` for rigid-body dynamics, and OpenMP for parallel computing. FDDP and iLQR consider the non-lifted contact dynamics based on Baumgarte’s stabilization method of the form in (8) as well as DMS-CD.

We set the weight parameters in Baumgarte’s stabilization method (5) as $\alpha = \beta = 25$. We approximated the contact position constraints (4) using a quadratic penalty function for simplicity. DMS-LCD and DMS-CD did not use any regularization on the Hessian and used only the fraction-to-boundary-rule [22] for the step-size selection. FDDP and iLQR used an adaptive regularization on the Hessian and a line-search based on the Goldstein condition in the step-size selection, as provided in the `Crocodyl` solver. We

¹Our open-source implementation of DMS-LCD is available online at <https://github.com/mayataka/idocep>

TABLE I
SETTINGS OF THE OCPs FOR THE FIVE QUADRUPEDAL GAITS

	Walking	Trotting	Pacing	Bounding	Jumping
N	107	57	71	71	71
$\Delta\tau$	0.02	0.02	0.01	0.01	0.01

conducted all the experiments for the two barrier parameters ϵ : $\epsilon = 1.0 \times 10^{-1}$ and $\epsilon = 1.0 \times 10^{-4}$, which represent a large and small barrier parameter, respectively. We set the relaxation parameter of the ReB for each ϵ and each gait as large as possible while keeping the optimal solution satisfying (36), which means that the “ideal” ReB was considered in the experiments. All experiments were conducted on a desktop computer with an octa-core CPU Intel Core i9-9900 @3.10 GHz, and all the algorithms were compiled using the GCC compiler with `-O3 -DNDEBUG -march=native` options. We used eight threads in parallel computing in this experiment.

B. Results and discussion

Fig. 1 shows \log_{10} scaled l_2 -norms of the KKT residuals with respect to the number of iterations of DMS-LCD (the proposed method), DMS-CD, FDDP, and iLQR over the five quadrupedal gaits with the barrier parameters $\epsilon = 1.0 \times 10^{-1}$ and $\epsilon = 1.0 \times 10^{-4}$. As shown in Fig. 1, the four methods resulted in a similar convergence when the barrier parameter was large ($\epsilon = 1.0 \times 10^{-1}$). In contrast, when the barrier parameter was small ($\epsilon = 1.0 \times 10^{-4}$), the proposed DMS-LCD converged significantly faster than the other methods, particularly in the aggressive gaits (pacing, bounding, and jumping). This is because, in the interior-point methods, a smaller barrier parameter (i.e., a more accurate solution) corresponds to a slower and more difficult convergence due to the high nonlinearity [23]. Nevertheless, the proposed method achieved fast convergence even with the small barrier parameter.

Fig. 2 shows the CPU time per iteration and the total CPU time until convergence of DMS-LCD, DMS-CD, FDDP, and iLQR over the five quadrupedal gaits. First, we observed that the CPU times per iteration of DMS-LCD and DMS-CD were almost identical and 1.6 to 2 times faster than those of FDDP and iLQR. This was because DMS could leverage parallel computing in the computation of the KKT residual, whereas single shooting methods such as FDDP and iLQR required to compute the contact dynamics (8) and impulse dynamics (13) over the horizon in serial computation. We compared the total computational time, and DMS-LCD had the fastest computational time in all the scenarios. It was more than twice as fast as the other methods in several scenarios. Fig. 3 shows the snapshots of the solution trajectory of the jumping gait ², and Fig. 4 shows the time histories of the contact forces of the four feet in the jumping gait. Both figures show that the friction cone constraints (36) were

²The supplemental video including the five gaits is available at <https://youtu.be/VgnWkgyIq-U>

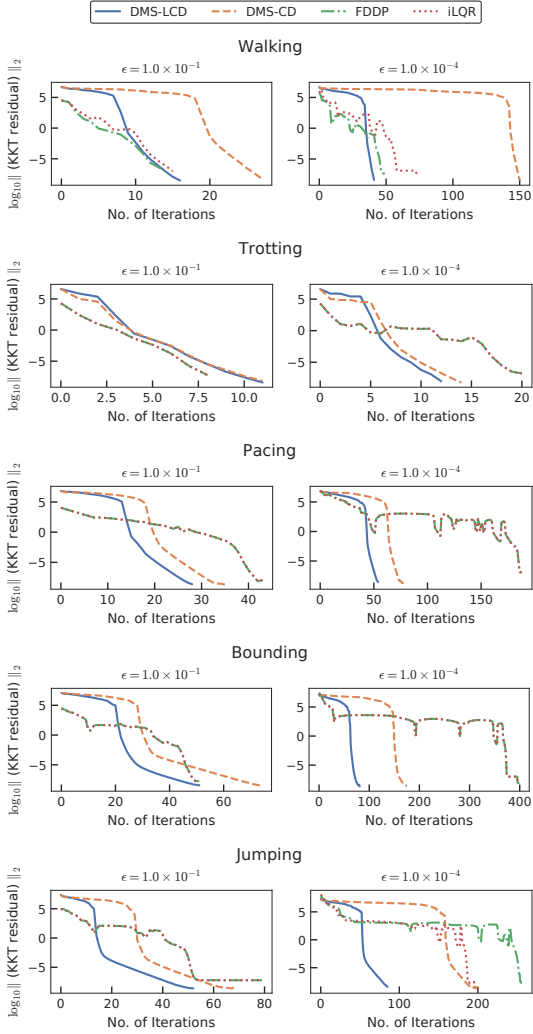


Fig. 1. \log_{10} scaled l_2 -norms of the KKT residuals of DMS-LCD (solid lines), DMS-CD (dashed lines), FDDP (dash-dotted lines), and iLQR (dotted lines) over the five quadrupedal gaits subject to the friction cone inequality constraints considered in the interior-point methods with the fixed barrier parameters $\epsilon = 1.0 \times 10^{-1}$ and $\epsilon = 1.0 \times 10^{-4}$.

active and the solution satisfied the constraints (36) in the jumping gait.

We further conducted several experiments with the various Baumgarte’s weight parameters $\alpha = \beta > 0$ in (5), the details of which are omitted here owing to the space limitation. We observed that as the weight parameter increased, the proposed method had greater advantages in terms of the convergence speed. In contrast, if the weight parameter was small, the proposed method had no such advantages. Note that a larger weight parameter typically results in a more accurate solution in terms of the original contact position constraints (4). This observation confirms that the proposed method can address high nonlinearity because the large Baumgarte’s weight parameters cause high nonlinearity in the contact dynamics (8) [19].

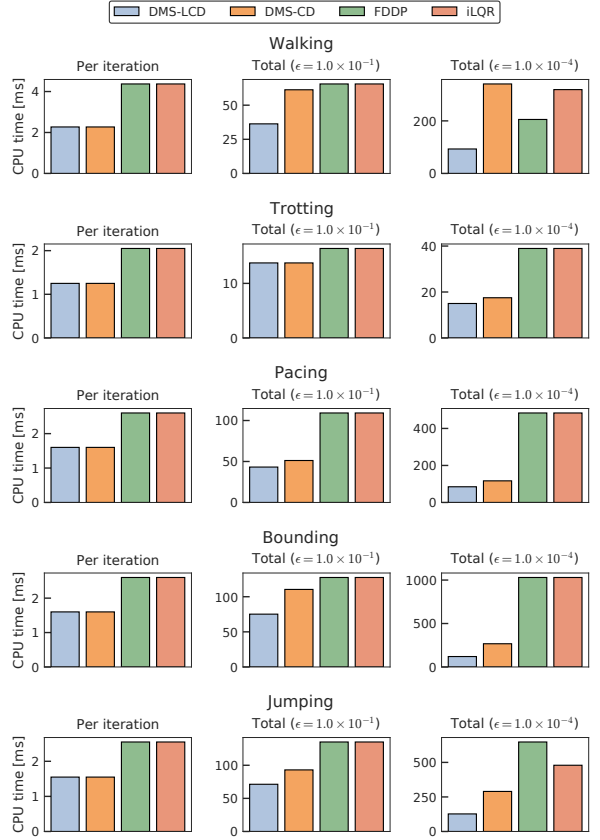


Fig. 2. CPU time per iteration and the total CPU time until convergence of DMS-LCD, DMS-CD, FDDP, and iLQR over the five quadrupedal gaits subject to the friction cone inequality constraints considered in the interior-point methods with the fixed barrier parameters $\epsilon = 1.0 \times 10^{-1}$ and $\epsilon = 1.0 \times 10^{-4}$.

V. CONCLUSIONS

We proposed a novel lifting approach for direct optimal control of rigid-body systems with contacts to improve the convergence properties of Newton-type methods. To relax the high nonlinearity, we considered all variables, including the state, acceleration, contact forces, and control input torques, as the optimization variables and the inverse dynamics and acceleration-level contact constraints as equality constraints. We eliminated the update of the acceleration, contact forces, and their dual variables from the linear equation to be solved in each Newton-type iteration in an efficient manner. As a result, the computational cost per Newton-type iteration is almost identical to that of the conventional non-lifted Newton-type iteration that embeds contact dynamics in the state equation. We conducted numerical experiments on the whole-body optimal control of various quadrupedal gaits subject to the friction cone constraints considered in the interior-point methods and demonstrated that the proposed method can significantly increase the convergence speed to more than twice that of the conventional non-lifted approaches. A future research direction is to combine the proposed method with the switching-time optimization methods [7], [8] to study real-time whole-body MPC for legged robots.

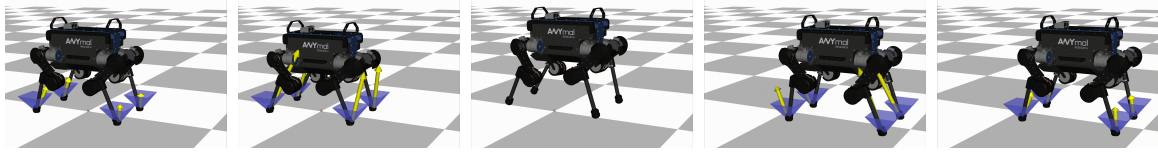


Fig. 3. Snapshots of the whole-body optimal control of the jumping motion of ANYmal subject to the friction cone constraints. The contact forces are indicated by the yellow arrows and linearized friction cones by the blue polyhedrons.

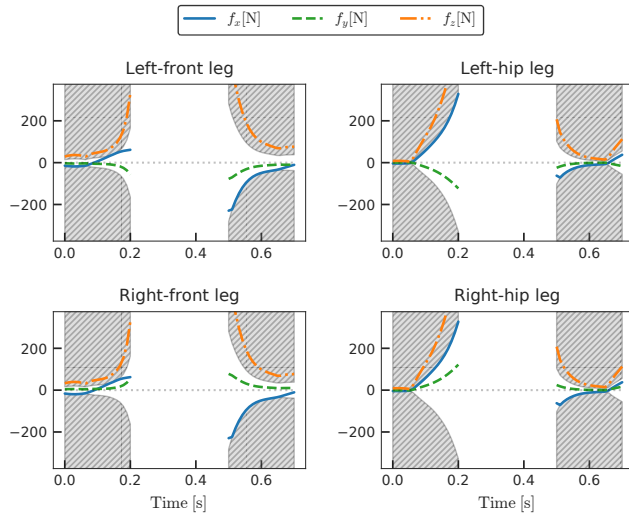


Fig. 4. Time histories of the contact force expressed in the world frame $[f_x \ f_y \ f_z]$ of each leg in the jumping motion. The infeasible regions of f_x and f_y due to the friction cone constraints (36) are the filled gray hatches. The infeasible region of $f_z \geq 0$ is the lower-half space of each plot.

REFERENCES

- [1] M. Neunert, M. Stauble, M. Gifthaler, C. D. Bellicoso, J. Carius, C. Gehring, M. Hutter, and J. Buchli, “Whole-body nonlinear model predictive control through contacts for quadrupeds,” *IEEE Robotics and Automation Letters*, vol. 3, no. 3, pp. 1458–1465, 2018.
- [2] I. Chatz Nikolaidis, Y. You, and Z. Li, “Contact-implicit trajectory optimization using an analytically solvable contact model for locomotion on variable ground,” *IEEE Robotics and Automation Letters*, vol. 5, no. 4, pp. 6357–6364, 2020.
- [3] D. E. Stewart and J. C. Trinkle, “An implicit time-stepping scheme for rigid body dynamics with inelastic collisions and Coulomb friction,” *International Journal for Numerical Methods in Engineering*, vol. 39, no. 15, pp. 2673–2691, 1996.
- [4] M. Posa, C. Cantu, and R. Tedrake, “A direct method for trajectory optimization of rigid bodies through contact,” *The International Journal of Robotics Research*, vol. 33, no. 1, pp. 69–81, 2014.
- [5] J. Carius, R. Ranftl, V. Koltun, and M. Hutter, “Trajectory optimization with implicit hard contacts,” *IEEE Robotics and Automation Letters*, vol. 3, no. 4, pp. 3316–3323, 2018.
- [6] A. Nurkanovic, S. Albrecht, and M. Diehl, “Limits of MPC formulations in direct optimal control with nonsmooth differential equations,” in *2020 European Control Conference (ECC)*, 2020, pp. 2015–2020.
- [7] S. Katayama, M. Doi, and T. Ohtsuka, “A moving switching sequence approach for nonlinear model predictive control of switched systems with state-dependent switches and state jumps,” *International Journal of Robust and Nonlinear Control*, vol. 30, no. 2, pp. 719–740, 2020.
- [8] H. Li and P. M. Wensing, “Hybrid systems differential dynamic programming for whole-body motion planning of legged robots,” *IEEE Robotics and Automation Letters*, vol. 5, no. 4, pp. 5448–5455, 2020.
- [9] G. Schultz and K. Mombaur, “Modeling and optimal control of human-like running,” *IEEE/ASME Transactions on Mechatronics*, vol. 15, no. 5, pp. 783–792, 2010.
- [10] R. Budhiraja, J. Carpentier, C. Mastalli, and N. Mansard, “Differential dynamic programming for multi-phase rigid contact dynamics,” in *IEEE-RAS International Conference on Humanoid Robots (ICHR)*, 2018.
- [11] C. Mastalli, R. Budhiraja, W. Merkt, G. Saurel, B. Hammoud, M. Naveau, J. Carpentier, L. Righetti, S. Vijayakumar, and N. Mansard, “Crocodyl: An efficient and versatile framework for multi-contact optimal control,” in *IEEE International Conference on Robotics and Automation (ICRA)*, 2020, pp. 2536–2542.
- [12] H. Bock and K. Plitt, “A multiple shooting algorithm for direct solution of optimal control problems,” in *9th IFAC World Congress*, 1984, pp. 1603–1608.
- [13] E. Todorov and W. Li, “A generalized iterative LQG method for locally-optimal feedback control of constrained nonlinear stochastic systems,” in *Proceedings of the 2005, American Control Conference*, 2005, pp. 300–306.
- [14] J. Carpentier and N. Mansard, “Analytical derivatives of rigid body dynamics algorithms,” in *Robotics: Science and Systems (RSS 2018)*, 2018, pp. hal-01790971v2f.
- [15] J. Albersmeyer and M. Diehl, “The lifted Newton method and its application in optimization,” *SIAM Journal on Optimization*, vol. 20, no. 3, pp. 1655–1684, 2010.
- [16] S. Katayama and T. Ohtsuka, “Efficient solution method based on inverse dynamics for optimal control problems of rigid body systems,” in *IEEE International Conference on Robotics and Automation (ICRA)*, 2021, p. 3029.
- [17] J. Sola, J. Deray, and D. Atchuthan, “A micro Lie theory for state estimation in robotics,” arXiv:1812.01537, 2020.
- [18] J. Baumgarte, “Stabilization of constraints and integrals of motion in dynamical systems,” *Computer Methods in Applied Mechanics and Engineering*, vol. 1, no. 1, pp. 1–16, 1972.
- [19] P. Flores, M. Machado, E. Seabra, and M. Silva, “A parametric study on the Baumgarte stabilization method for forward dynamics of constrained multibody systems,” *Journal of Computational and Nonlinear Dynamics*, vol. 6, p. 011019, 2011.
- [20] R. Featherstone, *Rigid Body Dynamics Algorithms*. Springer, 2008.
- [21] G. Frison, “Algorithms and methods for high-performance model predictive control,” Ph.D. dissertation, Technical University of Denmark, 2016.
- [22] A. Wachter and L. Biegler, “On the implementation of an interior-point filter line-search algorithm for large-scale nonlinear programming,” *Mathematical Programming*, vol. 106, pp. 25–57, 2006.
- [23] J. Nocedal and S. J. Wright, *Numerical Optimization*, 2nd ed. Springer, 2006.
- [24] M. Hutter, C. Gehring, A. Lauber, F. Gunther, C. D. Bellicoso, V. Tsounis, P. Fankhauser, R. Diethelm, S. Bachmann, M. Bloesch, H. Kolvenbach, M. Bjelonic, L. Isler, and K. Meyer, “ANYmal - toward legged robots for harsh environments,” *Advanced Robotics*, vol. 31, no. 17, pp. 918–931, 2017.
- [25] J. Hauser and A. Saccon, “A barrier function method for the optimization of trajectory functionals with constraints,” in *Proceedings of the 45th IEEE Conference on Decision and Control*, 2006, pp. 864–869.
- [26] J. Carpentier, G. Saurel, G. Buondonno, J. Mirabel, F. Lamiroux, O. Stasse, and N. Mansard, “The Pinocchio C++ library – A fast and flexible implementation of rigid body dynamics algorithms and their analytical derivatives,” in *International Symposium on System Integration (SII)*, 2019, pp. 614 – 619.
- [27] L. Dagum and R. Menon, “OpenMP: An industry-standard API for shared-memory programming,” *IEEE Computational Science & Engineering*, vol. 5, no. 1, p. 46–55, 1998.